

Supporting information

Removal of Intermediate Aromatic Halogenated DBPs by Activated Carbon Adsorption: A New Approach to Controlling Halogenated DBPs in Chlorinated Drinking Water

Jingyi Jiang, Xiangru Zhang*, Xiaohu Zhu and Yu Li

Department of Civil and Environmental Engineering, Hong Kong University of Science and Technology, Hong Kong, China

*Corresponding author phone: +852 23588479; fax: +852 23581534; e-mail: xiangru@ust.hk.

This supporting information including 25 pages, 8 tables, and 11 figures.

Contents of the Supporting Information

- 1. Design of RSSCT and Operational Concerns**
- 2. Chlorination of the RSSCT Effluent Samples with the Traditional Approach**
- 3. DBP Controlling with the New and Traditional Approaches with Coagulation**
- 4. Detection of THM₄**
- 5. Detection of HAA₉**
- 6. Detection of Polar Halogenated DBPs**
- 7. Bioassay Method**
- 8. References**

Table S1. Operation parameters of the large column and the RSSCT column.

Table S2. Chlorine doses and CT values of the bromide-containing effluent samples with the traditional approach.

Table S3. Chlorine doses and CT values of the bromide-free effluent samples with the traditional approach.

Table S4. Chlorine residuals in the 1-d subsequently chlorinated bromide-containing effluent samples with the traditional and new approaches.

Table S5. Characteristics of the influents with the new and traditional approaches.

Table S6. Molecular ion m/z values, UPLC RTs, and log P values of polar brominated DBPs detected in the bromide-containing influent and effluent samples with the new and traditional approaches.

Table S7. Molecular ion m/z values, UPLC RTs, and log P values of polar chlorinated DBPs detected in the bromide-free influent and effluent samples with the new and traditional approaches.

Table S8. Characteristics of the 1-d subsequently chlorinated bromide-containing raw water (the control sample).

Figure S1. Column reproducibility test results with virgin Calgon F300 and SRNOM (3 mg/L as C). Lines show logarithmic fits to the data for the comparison purpose.

Figure S2. TOX levels in (a) non-coagulated and (b) coagulated raw water samples with chlorination only (control), with the traditional approach, and with the new approach.

Figure S3. ESI-tqMS PIS spectrum of m/z 79 of the bromide-containing influent sample with the new approach. “ $\times 2$ ” indicates that the spectrum in m/z range of 100–200 was magnified by 2 times and “ $\times 5$ ” indicates that the spectrum in m/z range of 220–450 was magnified by 5 times.

Figure S4. TII values of bromide-containing effluents with the new and traditional approaches. To reflect all the polar brominated DBPs, TII value was calculated through the summation of ion intensity from m/z 80 to 600 in the ESI-tqMS PIS spectrum of m/z 79.

Figure S5. ESI-tqMS PIS spectrum of m/z 35 of the bromide-free influent sample with the new approach. “ $\times 2$ ” indicates that the spectrum in m/z range of 220–450 was magnified by 2 times.

Figure S6. ESI-tqMS PIS spectra of m/z 35 of the bromide-free effluent samples with the traditional approach collected at (a) 800 BVs, (b) 2000 BVs, (c) 4500 BVs, (d) 8000 BVs, and (e) 10750 BVs,

respectively; ESI-tqMS PIS spectra of m/z 35 of the bromide-free effluent samples with the new approach collected at (f) 800 BVs, (g) 2000 BVs, (h) 4500 BVs, (i) 8000 BVs, and (j) 10750 BVs, respectively. The y-axes are on the same scale with a maximum intensity of 6.40×10^5 . “ $\times 2$ ” in charts a–j indicates that the spectra in m/z range of 100–200 were magnified by 2 times and “ $\times 3$ ” in charts a–j indicates that the spectra in m/z range of 220–400 were magnified by 3 times.

Figure S7. TII values of bromide-free effluents with the new and traditional approaches. To reflect all the polar chlorinated DBPs, TII value was calculated through the summation of ion intensity from m/z 36 to 600 in the ESI-tqMS PIS spectrum of m/z 35.

Figure S8. Normalized peak areas of (a) 3-bromo-5-chloro-4-hydroxybenzaldehyde, (b) 3,5-dibromo-4-hydroxybenzaldehyde, (c) 3,5-dibromo-4-hydroxybenzoic acid, (d) 3,5-dibromosalicylic acid, (e) 2,4,6-tribromophenol, (f) 2,6-dibromo-1,4-hydrobenzoquinone, and (g) 2,6-dibromo-4-nitrophenol in the UPLC/ESI-tqMS MRM chromatograms of the bromide-containing effluent samples with the traditional approach (\diamond) and the new approach (\circ).

Figure S9. Normalized peak areas of (a) 3,5-dichloro-4-hydroxybenzaldehyde, (b) 2,4,6-trichlorophenol, (c) 3,5-dichloro-4-hydroxybenzoic acid, (d) 3,5-dichlorosalicylic acid, and (e) 2,6-dichloro-4-nitrophenol in the UPLC/ESI-tqMS MRM chromatograms of the bromide-free effluent samples with the traditional approach (\diamond) and the new approach (\circ).

Figure S10. The free chlorine residual decay curves of the bromide-containing and bromide-free influents.

Figure S11. The breakthrough profiles of DOC level in the effluent samples with the traditional approach (\diamond) and the new approach (\circ): (a) treatment of the bromide-containing simulated raw water, and (b) treatment of the bromide-free simulated raw water.

1. Design of RSSCT and Operational Concerns

1.1 Preparation of GAC Particles and Column. The RSSCT was conducted to simulate the performance of a pilot or full-scale column (large column) packed with virgin Calgon F300. To obtain small GAC particles used in the RSSCTs, the commercially GAC particles were grounded with pestle and mortar, and subjected to mechanical sieve. The carbon fraction with particle sizes of 170–230 mesh (with a mean particle diameter of 76 μm) was washed with ultrapure water and dried overnight to constant weight under 105 °C. The dried carbon was then stored in a desiccator until use. The GAC columns used in the RSSCTs were prepacked with the prepared GAC particles following the guidelines of Information Collection Rule (ICR) Manual of U.S. EPA.¹

1.2 Design of RSSCT. To design the RSSCTs, operating parameters of a typical pilot-scale fixed-bed GAC filter (i.e., large column) were assumed as shown in Table S1. In the column design part, the subscript LC stands for large column and SC stands for small column. Here shows the details of the system design:

(1) A scaling factor (SF) was determined first. The SF is defined as the ratio of particle diameter of large column (d_{LC}) to that of small column (d_{SC}) as described by the equation (S1). In this study, the mean particle diameter of large column was 1.10 mm, and that of small column was 0.076 mm. Using the Equation S1, the following SF was yielded.

$$SF = \frac{d_{LC}}{d_{SC}} = \frac{1.10 \text{ mm}}{0.076 \text{ mm}} = 14.47 \quad (\text{S1})$$

(2) Using the proportional diffusivity (PD) scaling approach¹ with an assumption that the surface diffusion coefficient (D_s) of a DBP or other organic compound is a linear function of GAC particle diameter ($X=1$), the following equation was used to calculate the empty bed contact time (EBCT) of the small column (EBCT_{SC}):

$$\frac{\text{EBCT}_{SC}}{\text{EBCT}_{LC}} = \left(\frac{d_{SC}}{d_{LC}}\right)^{2-X} = \left(\frac{d_{SC}}{d_{LC}}\right) = \frac{1}{SF} \quad (\text{S2})$$

Since EBCT_{LC} was assumed to be 10 min, the EBCT_{SC} was calculated as follows:

$$\text{EBCT}_{SC} = \frac{\text{EBCT}_{LC}}{SF} = \frac{10.0 \text{ min}}{14.47} = 0.691 \text{ min}$$

(3) The hydraulic loading rate in the small column (V_{SC}) is also directly related to the hydraulic loading rate in the large column (V_{LC}) by the scaling factor as follows:

$$\frac{V_{SC}}{V_{LC}} = \left(\frac{d_{LC}}{d_{SC}} \right) \times \frac{Re_{SC}}{Re_{LC}} = SF \quad (S3)$$

where V is the hydraulic loading rate; Re is the Reynolds number.

The design of the small column using Equations S2 and S3 can yield the small column with the same length as the large column as shown in the Equation S4. However, a significant increase of head loss can also occur in the small column due to the rather small inner diameter in comparison with the large column.

$$l_{SC} = V_{SC} \times EBCT_{SC} = (V_{LC} \times SF) \times \left(\frac{EBCT_{LC}}{SF} \right) = V_{LC} \times EBCT_{LC} = l_{LC} \quad (S4)$$

To solve this, the dominance of internal mass transfer over external mass transfer was utilized. The Reynolds number in the small column (Re_{SC}) does not impact the breakthrough curve as long as internal mass transfer dominates external mass transfer.² The minimum velocity in the small column is defined using the minimum Reynolds number ($Re_{sc,min}$). According to the U.S. EPA's ICR Manual,¹ the $Re_{sc,min}$ is recommended to range between 0.5 and 1.0.

$$\frac{V_{SC}}{V_{LC}} = \left(\frac{d_{LC}}{d_{SC}} \right) \times \frac{Re_{SC,min}}{Re_{LC}} \quad (S5)$$

$$Re = \frac{V \times d_p}{\varepsilon \times \nu} \quad (S6)$$

$$V_{SC} = \frac{Re_{SC,min}}{Re_{LC}} \times SF \times V_{LC} = \frac{Re_{SC,min} \times \nu_{LC} \times \varepsilon_{LC}}{d_{SC}} \quad (S7)$$

where ν_{LC} is the kinematic viscosity of water ($1.004 \times 10^{-2} \text{ cm}^2/\text{s}$, at ambient temperature, 20 °C); ε_{LC} is the GAC bed porosity.

The $Re_{sc,min}$ was assumed to be 0.54 and the bed porosity of the large column was assumed to be 0.421. V_{SC} was calculated as follows:

$$V_{SC} = \frac{0.54 \times 1.004 \times 10^{-2} \frac{\text{cm}^2}{\text{s}} \times 0.421}{0.076 \text{ mm}} \times \frac{60 \text{ s}}{\frac{1 \text{ min}}{\frac{1 \text{ cm}}{10 \text{ mm}}}} = 18.02 \text{ cm/min}$$

(4) The bed depth of the small column (l_{SC}) was calculated as follows:

$$l_{SC} = V_{SC} \times EBCT_{SC} = 18.02 \frac{\text{cm}}{\text{min}} \times 0.691 \text{ min} = 12.45 \text{ cm}$$

(5) The inner diameter of the glass column (D_{SC}) used for the RSSCT was 7.0 mm (0.7 cm). To avoid channeling, the ratio of column inner diameter to GAC particle diameter must be greater than 50. Because the d_{SC} was 0.076 mm, the D_{SC} was suitable for the RSSCT operation.

$$D_{SC} > 50 d_{SC} = 50 \times 0.076 \text{ mm} = 3.8 \text{ mm} \quad (\text{S8})$$

The flow rate of the small column (Q_{SC}) was calculated as follows:

$$Q_{SC} = v_{SC} \times \pi \times \frac{D_{SC}^2}{4} = 18.02 \frac{\text{cm}}{\text{min}} \times \pi \times \frac{(0.7 \text{ cm})^2}{4} = 6.93 \text{ cm}^3/\text{min} = 6.93 \text{ mL/min} \quad (\text{S9})$$

(6) As the density of Calgon F300 is 0.45 g/cm³ (ρ_{SC}), the mass of GAC needed for the RSSCT (m_{SC}) was calculated as:

$$m_{SC} = l_{SC} \times \rho_{SC} \times \pi \times \frac{D_{SC}^2}{4} = 12.45 \text{ cm} \times 0.45 \frac{\text{g}}{\text{cm}^3} \times \pi \times \frac{(0.7 \text{ cm})^2}{4} = 2.155 \text{ g} \quad (\text{S10})$$

(7) To estimate the minimum volume of influent water needed for the RSCCT (Vol_{SC}), empirical equations can be used to predict GAC bed breakthrough according to the influent TOC level. Calgon F300 is a bituminous coal-based GAC, so the Equation S11 was adopted here.² Accordingly, for the influent TOC level of 3 mg/L, the bed volumes (BVs) at 50% breakthrough was obtained as:

$$BV_{50\%} = 21700 \times TOC_0^{-1.3} = 5202.4 \text{ BVs} \quad (\text{S11})$$

The total run time of the RSSCT, t_{SC}^T , was calculated as:

$$t_{SC}^T = 2 \times BV_{50} \times EBCT_{SC} = 2 \times 5202.4 \text{ BVs} \times 0.691 \text{ min} \times \frac{1 \text{ d}}{1440 \text{ min}} = 4.99 \text{ d} \quad (\text{S12})$$

Thus, Vol_{SC} of influent water needed for the RSCCT was calculated as:

$$Vol_{SC} = Q_{SC} \times t_{SC}^T = 6.93 \frac{\text{mL}}{\text{min}} \times 4.99 \text{ d} \times \frac{1440 \text{ min}}{1 \text{ d}} \times \frac{1 \text{ L}}{1000 \text{ mL}} = 49.80 \text{ L} \quad (\text{S13})$$

(8) During the RSSCT operation, the run time was extended to around 12000 BVs to ensure that the GAC reached a complete breakthrough.

1.3 Reproducibility Tests. Since a single RSSCT operation could not provide enough samples for both chemical and biological analyses, parallel RSSCT operations were conducted. Because there were non-quantifiable factors that could impact the DOC breakthrough patterns of parallel RSSCTs, (such as the variability in sampling glassware cleanness, the variability in the analytical measurements from day-to-day operation, the fluctuations in flow rate and pressure change during long experiment period, and differences in column packing), the reproducibility of breakthrough patterns were evaluated. The bromide-containing and bromide-free simulated raw waters were fed to parallel RSSCTs using the virgin Calgon F300. For one raw water, duplicate RSSCTs were conducted (Tests 1 and 2 in Figure S1). The four DOC breakthrough curves are shown in Figure S1. The results showed good reproducibility. Logarithmic equations were fitted to the experimental data and the variability of four breakthrough curves was calculated at the same BVs. The relative standard deviation of DOC was within 5–10%. These results indicated that using the experimental setups in this study obtained reproducible results from parallel RSSCTs. Therefore, results obtained from different batches of RSSCTs can be compared.

2. Chlorination of the RSSCT Effluent Samples with the Traditional Approach

The CT value is used to determine or predict the germicidal efficiency of disinfection. It is defined as the product of the residual disinfectant concentration (C) in mg/L, and the contact time (T) in min.³ As the CT value increases, a higher percentage of microorganisms are inactivated by the chemical disinfection. The CT value, which is positively correlated with the level of inactivation, can be increased by applying a higher dose of the disinfectant or by increasing the time that the water is in contact with the disinfectant.

In this study, a same CT value was applied to ensure the same disinfection efficiency with the new and traditional approaches. The bromide-containing or bromide-free simulated raw water (pH 8.5) dosed with 5 mg/L NaOCl as Cl₂ for a 30-min contact time in darkness was used as a control to obtain a reference CT value. The reaction conditions of the control sample were equivalent to those with the new approach. With the DPD colorimetric method,⁴ the free chlorine residual decay curves of the two raw waters were obtained, which are shown in Figure S9. The reference CT value of each water was quantified as the area under the corresponding free

chlorine residual curve in Figure S9.

For the effluent samples with the traditional approach, their DOC levels gradually increased along with the column operation. It has been reported that the chlorine demand of a water sample is somewhat related to the sample DOC level.³ Thus, to maintain the same CT value as the reference value for the effluent samples, various chlorine doses were set based on the DOC levels in the effluent samples. For each effluent sample, the chlorine contact time was kept at 30 min and the chlorination was conducted in darkness at room temperature. The CT values, DOC levels, pH values and the corresponding chlorine doses of the bromide-containing and bromide-free effluent samples were summarized in Tables S2 and S3.

3. DBP Controlling with the New and Traditional Approaches with Coagulation

3.1 Coagulation of the Simulated Raw Water. Jar tests were conducted for coagulation using a Stuart SW6 flocculator (Cole-Parmer, UK). Jars were 1-L silanized glass beakers, each filled with 0.5 L of the simulated bromide-containing raw water (initial pH 8.5). Aluminum sulfate (alum, $\text{Al}_2(\text{SO}_4)_3 \cdot 14\text{H}_2\text{O}$) was used as coagulant. An alum dose (10 mg of alum/ mg of TOC) was selected on the basis of the TOC concentration of the water and represents the high end of dosages that may be used to meet the U.S. EPA Interim Enhanced Surface Water Treatment Rule.⁵ Alum was added to the test solution via pipette prior to the rapid mixing. Mixing conditions were kept the same as the ones adopted in a previous study because the same water matrix was used in the previous study.⁶ In brief, mixing conditions were 1-min of rapid mixing at 100 rpm, 20-min of flocculation at 30 rpm, and 60-min of settling. The jar tests were conducted at a room temperature of 20 ± 1 °C. After settling, supernatant samples were collected and transferred via glass pipette to a 2-L Teflon-lined amber glass bottle for further experiment.

3.2 DBP Removals with the New and Traditional Approaches with Coagulation. The simulated bromide-containing raw water without or with coagulation was treated with the new or traditional approach. Micro-column adsorption tests using a commercially available activated carbon column (TXAPPC, Mitsubishi, Japan) were conducted to simulate the performance of a GAC filter in both approaches. For the new approach, the simulated raw water sample without or with coagulation was chlorinated by dosing 5 mg/L NaOCl as Cl_2 in the dark at room temperature for a contact time of 30 min and then passed through the activated carbon column. For the traditional approach, the simulated raw water sample without or with coagulation passed

through the activated carbon column and then were chlorinated under the same CT condition as the new approach. The contact time (30 min) was kept the same. A control sample was prepared by chlorinating the simulated raw water sample without or with coagulation by dosing 5 mg/L NaOCl as Cl_2 in the dark at room temperature for a contact time of 30 min. After a given contact time, the chlorine residual in each chlorinated sample was quenched with $\text{Na}_2\text{S}_2\text{O}_3$. Then, TOX in the effluent and control samples was measured.

Figure S2a shows the TOX levels in the non-coagulated bromide-containing raw water samples with chlorination only (control), with the traditional approach, and with the new approach. Figure S2b shows the TOX levels in the coagulated bromide-containing raw water samples with chlorination only, with the traditional approach, and with the new approach. Compared with the non-coagulated bromide-containing raw water sample with chlorination only (control), coagulation removed only 9.9% of TOX, coagulation with the traditional approach removed 33.9% of TOX, and coagulation with the new approach removed 63.6% of TOX. The results indicated that even with coagulation, the new approach also showed a significantly better control of overall halogenated DBPs than the traditional approach.

4. Detection of THM₄

THMs were extracted and analyzed following the modified U.S. EPA Method 551.1. In brief, 3 mL pentane and 6 g Na_2SO_4 were added into a 30-mL sample. The sample was shaken vigorously for 4 min and was allowed to settle for another 2 min. After stabilization, the upper pentane layer was transferred to a 1.8-mL auto-sampler vial and sealed with a Teflon-lined cap for the detection of THMs by gas chromatography with an electron capture detector (7890A, Agilent). An HP-5MS capillary column (30 m \times 0.25 mm with 0.25 μm film thickness, Agilent J&W GC Columns) was used to separate THMs under the following procedure: a hold at 35°C for 5 min, a ramp to 80 °C at 4 °C/min, a ramp to 110 °C at 20 °C/min, a hold at 110 °C for 8.5 min, a ramp to 180 °C at 40 °C/min, followed by a hold at 180 °C for 1 min. To determine THM concentrations in the effluent samples, a series of standard solutions for calibration (within the range of 1–500 $\mu\text{g/L}$ for each THM) were prepared by diluting the standard THM₄ mixture (2000 mg/L for each species in methanol) with ultrapure water and were extracted and analyzed for THMs with the same procedure as aforementioned. A blank sample with ultrapure water only was pretreated with the aforementioned procedure and used as a control. For each effluent sample, duplicate aliquots were analyzed to obtain an average THM concentration and the

quantitation limit for each THM species was 0.5 $\mu\text{g/L}$ in a water sample.

5. Detection of HAA₉

HAAs were extracted, transformed into methyl acetates through derivatization and analyzed following the modified U.S. EPA Method 552.3. Briefly, a 30-mL sample was acidified with sulfuric acid to pH 0.5 and was saturated with 6 g of anhydrous Na_2SO_4 . The sample was then extracted with 4 mL of MtBE. After stabilization, 2.5 mL of MtBE was transferred into a 16-mL amber glass vial together with 2.5 mL acidic methanol (sulfuric acid: methanol (v/v) = 1:10). After mixing, the sample underwent a 2-h water bath at 50 °C for esterification. After esterification, the treated sample was kept at 4 °C for 5 min to cool down and then recovered to room temperature. An extra 7 mL of 10% Na_2SO_4 solution (Na_2SO_4 : ultrapure water (w/w) = 1:10) was added to separate MtBE and methanol, and another 4 mL of saturated NaHCO_3 solution was added to neutralize the pretreated acidic sample. After the extraction and stabilization, 1 mL MtBE layer was transferred into a 1.8-mL auto-sampler vial and sealed with a Teflon-lined cap for the detection of HAAs by gas chromatography with an electron capture detector (7890A, Agilent).

The nine halogenated methyl acetates were separated with an HP-5MS capillary column (30 m \times 0.25 mm with 0.25 μm film thickness, Agilent J&W GC Columns) under the following procedure: a hold at 40 °C for 5 min, a ramp to 55 °C at 5 °C/min, a ramp to 65 °C at 1 °C/min, a ramp to 85 °C at 10 °C/min, a ramp to 205 °C at 20 °C/min, followed by a hold at 205 °C for 5 min. To determine HAA concentrations in the effluent samples, a series of standard solutions for calibration (within the range of 1–250 $\mu\text{g/L}$ for each HAA) were prepared by diluting the standard HAA₉ mixture (2000 mg/L for each species in MtBE) with ultrapure water and were pretreated and analyzed for HAAs with the same procedures as aforementioned. A blank sample with ultrapure water only was pretreated with the aforementioned procedure and used as a control. For each effluent sample, duplicate aliquots were analyzed to obtain an average HAA concentration and the quantitation limit for each HAA species was 0.5 $\mu\text{g/L}$ in a water sample.

6. Detection of Polar Halogenated DBPs

ESI-tqMS PIS analysis was used for the selective detection of polar halogenated DBPs in the pretreated water sample. The ESI-tqMS instrumental parameters were optimized and set according to a previous study:⁷ ESI negative mode, sample flow rate via an infusion pump 10

$\mu\text{L}/\text{min}$, capillary voltage 2.8 kV, cone voltage 15 V for brominated DBPs and 30 V for chlorinated DBPs, cone gas flow 50 L/h, source temperature 120 °C, desolvation temperature 350 °C, desolvation gas flow 650 L/h, collision energy 30 eV for chlorinated DBPs and 20 eV for brominated DBPs, collision gas (argon) flow 0.25 mL/min, and mass resolution 15 (1-unit resolution). By setting ESI-tqMS PISs of m/z 79/81 (or m/z 35/37), all electrospray-ionizable brominated DBPs (or chlorinated DBPs) in a pretreated sample were detected. For PISs' data collection, multi-channel analysis mode was set to enhance precursor ion intensities by accumulating multiple scans (with a scan time of 0.3 s, run durations of 5 min for PISs m/z 79/81 and 7 min for PISs m/z 35/37, respectively) so that ion intensity fluctuation in a single scan could be avoided.

A UPLC system (Waters) was coupled with the ESI-tqMS for pre-separation. The UPLC separation was performed with an HSS T3 column (1.8 μm particle size, 100 \times 2.1 mm, Waters Corporation) at a column temperature of 35 °C. The injection volume was 7.5 μL . The mobile phase consisted of methanol and water and was applied at a flow rate of 0.4 mL/min. The methanol/water (v/v) gradient was set at 5/95 initially and changed linearly to 90/10 in the first 8.0 min. Within the next 0.1 min, it changed back to 5/95, which was held for additional 2.9 min. The MS parameters for the UPLC/ESI-tqMS were set the same as those for the ESI-tqMS with the exception of a higher desolvation temperature (400 °C) and a higher desolvation gas flow (800 L/h). For a molecular ion detected by PIS, the MRM mode with a dwell time of 0.05 s was applied to gain the retention time (RT) and the isotopic abundance ratio. To confirm the presence of a specific halogenated DBP in a pretreated sample, the corresponding standard compound and the sample spiked with the corresponding standard compound were analyzed with the same MRM mode.

With the UPLC/ESI-tqMS MRM analyses, the aromatic halo-DBPs listed in Tables S6 and S7 were selectively detected and confirmed by the corresponding standard compound. In the MRM chromatogram of an effluent sample, the area of a peak approximately reflects the level of the corresponding DBP in the sample. For instance, the level of 2,4,6-tribromophenol (m/z 327/331/333) in a sample was obtained from the peak area (with the RT of 7.99 min) in the UPLC/ESI-tqMS MRM (327 \rightarrow 79, 329 \rightarrow 79/81, 331 \rightarrow 79/81, 333 \rightarrow 81) chromatogram.

7. Bioassay Method

Stock cultures of *P. dumerilii* were maintained as described previously.^{8,9} Briefly, the polychaete

was cultured on a diet of algae, fish flakes and chopped spinach and held in the prepared seawater at 19 ± 1 °C. Breeding was controlled by photoperiod manipulation giving 16 h of light (at a light intensity of approximately 300 lux) followed by 8 h of absolute darkness.

Mature males and females were transferred from the culturing tanks and allowed to spawn naturally in approximately 50 mL of the seawater. Once fertilization was confirmed to be successful (routinely > 95%, as indicated by the first cellular cleavage), the developing embryos were transferred to an incubation glass basin containing 500 mL of the seawater for the developmental toxicity tests. After 12 h post-fertilization, the embryos of the polychaete *P. dumerilii* were collected and transferred to a 1.6-cm tissue culture test-plate that contained seawater (as a control) or a test sample (with a total volume of 2.0 mL). The embryos (approximately 75 embryos/mL) were allowed to develop for a further 12 h. By 24 h post-fertilization, normal embryos are expected to have reached the first larval (trochophore) stage, characterized by the presence of distinct ciliary bands, prominent fat droplets, and active swimming activity. Abnormal embryos lack some or all of these characteristics. The numbers of normal and total embryos in each test solution were checked with an inverted microscope (magnification by 40 times), and the percentage of embryos developing normally was calculated. A lower normal development percentage represents a higher comparative developmental toxic potency.

To compare the toxicity of raw water treated by the new and traditional approaches, preliminary experiments were conducted to obtain a suitable concentration factor (CF) for the pretreatment of the effluent samples. By concentrating all samples at a specific CF, the highest and lowest toxic effluent samples with either new or traditional approach could induce approximately 100% abnormal development and a significant amount of abnormal development (i.e., the normal development percentage is 5% less than the seawater control sample), respectively. In this study, CFs of 140 and 310 were selected for the toxicity evaluation of the bromide-containing and bromide-free effluent samples, respectively. For the evaluation of 1-d subsequently chlorinated bromide-containing effluent samples, a CF of 220 was used. By plotting the curve of the normal development percentage versus the corresponding sample collected at a specific BV of water treated, a response profile was obtained.

8. References

- (1) Westrick, J. J.; Allgeier, S. C. *ICR Manual for Bench- and Pilot-scale Treatment Studies*; U.S.

Environmental Protection Agency: Cincinnati, OH, 1996.

(2) Crittenden, J.; Berrigan, J. K.; Hand, D.; Lykins, B. Design of rapid fixed-bed adsorption tests for nonconstant diffusivities. *J. Environ. Eng.* **1987**, *113* (2), 243–259.

(3) Crittenden, J. C.; Trussell, R. R.; Hand, D. W.; Howe, K. J.; Tchobanoglous, G. *MWH's Water Treatment: Principles and Design*; John Wiley & Sons, Inc.: Hoboken, NJ, 2012.

(4) APHA; AWWA; WEF. *Standard Methods for the Examination of Water and Wastewater*; 22nd ed.; APHA: Washington, DC, 2012.

(5) U.S. EPA. *Interim Enhanced Surface Water Treatment Rule* (EPA 815-F-98-009); U.S. Environmental Protection Agency: Washington, DC, 1998.

(6) Westerhoff, P.; Yoon, Y.; Snyder, S.; Wert, E. Fate of endocrine-disruptor, pharmaceutical, and personal care product chemicals during simulated drinking water treatment processes. *Environ. Sci. Technol.* **2005**, *39* (17), 6649–6663.

(7) Liu, J.; Zhang, X.; Li, Y. Effect of boiling on halogenated DBPs and their developmental toxicity in real tap waters. In *Recent Advances in Disinfection By-products*; Karanfil, T., Mitch, B., Westerhoff, T., Xie, Y., Eds.; American Chemical Society: Washington, DC, 2015; pp 45–60.

(8) Hutchinson, T. H.; Jha, A. N.; Mackay, J. M.; Elliott, B. M.; Dixon, D. R. Assessment of developmental effects, cytotoxicity and genotoxicity in the marine polychaete (*Platynereis dumerilii*) exposed to disinfected municipal sewage effluent. *Mutat. Res., Fundam. Mol. Mech. Mutagen.* **1998**, *399* (1), 97–108.

(9) Yang, M.; Zhang, X. Comparative developmental toxicity of new aromatic halogenated DBPs in a chlorinated saline sewage effluent to the marine polychaete *Platynereis dumerilii*. *Environ. Sci. Technol.* **2013**, *47* (19), 10868–10876.

Table S1. Operation parameters of the large column and the RSSCT column.^a

Parameters	RSSCT	Large Column
GAC particle size (mesh size)	170×230	12×40
GAC diameter (mm)	0.076	1.1
Bed depth (cm)	12.45	300.0
Column inner diameter (mm)	7.0	600.0
Hydraulic loading rate (cm/min)	18.0	30.0
Volumetric flow rate (mL/min)	6.93	8.48×10 ⁴
Empty bed contact time (min)	0.691	10.0

^aThe scaling factor was 14.47.

Table S2. Chlorine doses and CT values of the bromide-containing effluent samples with the traditional approach.

BV	DOC (mg/L as C)	pH	Cl ₂ dose (mg/L)	CT (mg/L as Cl ₂ × min)
150	1.24	8.63	4.0	104.1
300	1.51	8.55	4.1	103.2
500	1.54	8.63	4.1	102.6
1200	1.68	8.53	4.2	103.8
2000	1.94	8.52	4.3	105.7
3000	2.31	8.45	4.6	100.5
4000	2.72	8.55	4.7	104.3
5250	2.89	8.52	4.8	100.5
6500	2.88	8.46	4.8	101.7
7750	2.94	8.61	5.0	103.7
9000	2.97	8.69	5.0	103.4
10500	3.04	8.47	5.0	100.4
12500	2.98	8.46	5.0	102.7
Reference ^a	3.08	8.63	5.0	103.4

^aThe reference CT value was the CT value of the influent with the new approach.

Table S3. Chlorine doses and CT values of the bromide-free effluent samples with the traditional approach.

BV	DOC (mg/L as C)	pH	Cl ₂ dose (mg/L)	CT (mg/L as Cl ₂ × min)
150	0.81	8.42	4.1	127.4
300	1.39	8.60	4.2	124.9
500	1.62	8.56	4.4	126.2
1200	2.15	8.43	4.6	127.4
2000	2.36	8.53	4.7	125.6
3000	2.51	8.60	4.8	120.8
4000	2.60	8.51	4.8	129.9
5250	2.65	8.53	4.8	131.9
6500	2.71	8.50	4.9	125.4
7750	2.78	8.59	4.9	132.1
9000	2.79	8.56	4.9	131.0
10250	2.85	8.61	4.9	129.8
11500	2.96	8.57	5.0	130.4
Reference ^a	3.05	8.49	5.0	129.8

^aThe reference CT value was the CT value of the influent with the new approach.

Table S4. Chlorine residuals in the 1-d subsequently chlorinated bromide-containing effluent samples with the traditional and new approaches.

BV	<u>Traditional approach</u>		<u>New approach</u>	
	Effluent sample (mg/L as Cl ₂) ^a	After 1-d chlorination (mg/L as Cl ₂)	Effluent sample (mg/L as Cl ₂) ^a	After 1-d chlorination (mg/L as Cl ₂)
300	2.72	1.57	2.72	1.25
1000	2.65	0.98	2.65	0.86
2500	2.58	0.83	2.58	0.47
4000	2.69	0.77	2.69	0.41
6500	2.55	0.76	2.55	0.36
9000	2.65	0.71	2.65	0.33
12000	2.60	0.68	2.60	0.23
Reference ^b	2.57	0.42		

^aFor the effluent samples with the traditional approach, the chlorine residuals were measured after a 30-min chlorination. For the new approach, the same level of chlorine was dosed back to the corresponding effluent samples to maintain a similar chlorine residual at the beginning of 1-d subsequent chlorination.

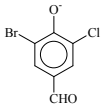
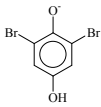
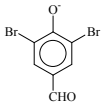
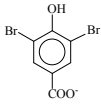
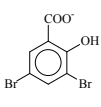
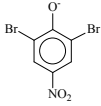
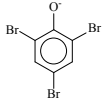
^bThe reference chlorine residual level was equivalent to the chlorine residual in the raw water dosed with 5 mg/L NaOCl as Cl₂ after a contact time of 30 min or “1 d + 30 min”.

Table S5. Characteristics of the influents with the new and traditional approaches.^a

Influent composition	<u>Bromide-containing influent</u>		<u>Bromide-free influent</u>	
	Traditional approach	New approach	Traditional approach	New approach
DOC (mg/L as C)	3.05 ± 0.04	3.08 ± 0.03	3.05 ± 0.04	3.05 ± 0.03
Trichloromethane, TCM (μg/L)	ND	ND	56.72 ± 1.70	56.14 ± 1.40
Bromodichloromethane, BDCM (μg/L)	5.30 ± 0.07	5.19 ± 0.04	ND	ND
Chlorodibromomethane, CDBM (μg/L)	28.11 ± 0.31	28.62 ± 0.35	ND	ND
Tribromomethane, TBM (μg/L)	134.22 ± 1.81	132.90 ± 1.61	ND	ND
THM ₄ (μg/L)	167.63 ± 2.19	166.71 ± 2.35	56.72 ± 1.70	56.14 ± 1.40
Monochloroacetic acid, MCAA (μg/L)	ND	ND	ND	ND
Monobromoacetic acid, MBAA (μg/L)	0.99 ± 0.08	1.11 ± 0.11	ND	ND
Dichloroacetic acid, DCAA (μg/L)	2.85 ± 0.02	2.68 ± 0.05	13.23 ± 0.31	13.28 ± 0.34
Trichloroacetic acid, TCAA (μg/L)	0.72 ± 0.01	0.61 ± 0.01	12.11 ± 0.05	12.58 ± 0.63
Dibromoacetic acid, DBAA (μg/L)	30.14 ± 0.02	30.33 ± 0.15	ND	ND
Bromochloroacetic acid, BCAA (μg/L)	8.38 ± 0.06	8.33 ± 0.15	ND	ND
Bromodichloroacetic acid, BDCAA (μg/L)	3.20 ± 0.19	3.47 ± 0.01	ND	ND
Dibromochloroacetic acid, DBCAA (μg/L)	4.93 ± 0.03	5.04 ± 0.07	ND	ND
Tribromoacetic acid, TBAA (μg/L)	22.54 ± 0.08	22.60 ± 0.24	ND	ND
HAA ₅ (μg/L)	34.71 ± 0.19	34.73 ± 0.60	25.35 ± 0.36	25.86 ± 0.67
HAA ₉ (μg/L)	73.76 ± 0.26	74.17 ± 1.08	25.35 ± 0.36	25.86 ± 0.67
TOCl (μg/L as Cl)	106.1 ± 5.2	100.7 ± 5.4	229.5 ± 9.2	231.0 ± 8.6
TOBr (μg/L as Cl)	194.8 ± 5.0	202.5 ± 2.3	ND	ND
TOX (μg/L as Cl)	300.9 ± 6.9	303.2 ± 6.1	229.5 ± 9.2	231.0 ± 8.6

^aThe influent DBP levels with the traditional approach represent the DBP levels in the influent which was chlorinated by dosing 5 mg/L NaOCl as Cl₂ for a 30 min contact time. “ND” means “not detected”, which indicates that the concentration was below the detection limit.

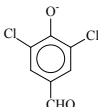
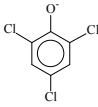
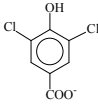
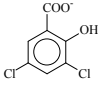
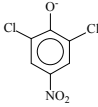
Table S6. Molecular ion m/z values, UPLC RTs, and log P values of polar brominated DBPs detected in the bromide-containing influent and effluent samples with the new and traditional approaches.

	m/z	Formula/ Structure	RT (min)	log P ^β
Aliphatic DBPs	127/129/131	ClBrCHCOO ^{-α}	0.82	1.084
	137/139	BrCH ₂ COO ⁻	0.71	0.511
	161/163/165/167	Cl ₂ BrCCOO ^{-α}	1.92	2.110
	171/173/175	ClBrCHCOO ⁻	0.82	1.084
	171/173/175	Br ₂ CHCOO ^{-α}	0.86	1.563
	205/207/209/211	Cl ₂ BrCCOO ⁻	1.92	2.110
	205/207/209/211	ClBr ₂ CCOO ^{-α}	2.10	2.548
	215/217/219	Br ₂ CHCOO ⁻	0.86	1.563
	249/251/253/255	Br ₃ CCOO ^{-α}	2.28	3.047
Aromatic DBPs	233/235/237		4.17	3.511
	265/267/269		6.76	2.210
	277/279/281		4.50	4.016
	293/295/297		3.33	3.858
	293/295/297		5.23	4.669
	294/296/298		5.34	3.607
	327/329/331/333		7.99	4.404

^αdecarboxylated at the sample cone of the ESI-tqMS;

^βdata collected from Scifinder database.

Table S7. Molecular ion m/z values, UPLC RTs, and log P values of polar chlorinated DBPs detected in the bromide-free influent and effluent samples with the new and traditional approaches.

	m/z	Formula/ Structure	RT (min)	log P ^β
Aliphatic DBPs	83/85/87	Cl ₂ CHCOO ⁻ ^α	0.82	0.667
	117/119/121/123	Cl ₃ CCOO ⁻ ^α	1.80	1.734
	127/129/131	Cl ₂ CHCOO ⁻	0.82	0.667
	161/163/165/167	Cl ₃ CCOO ⁻	1.80	1.734
Aromatic DBPs	189/191/193		4.13	2.827
	195/197/199/201		7.53	3.769
	205/207/209		3.27	3.369
	205/207/209		4.94	4.178
	206/208/210		5.01	2.914

^αdecarboxylated at the sample cone of the ESI-tqMS;

^βdata collected from Scifinder database.

Table S8. Characteristics of the 1-d subsequently chlorinated bromide-containing raw water (the control sample).

TCM (μg/L)	5.6±0.1	HAA ₅ (μg/L)	70.3±3.8
BDCM (μg/L)	5.9±0.1	BCAA (μg/L)	6.7±0.4
CDBM (μg/L)	47.3±1.4	BDCAA (μg/L)	3.3±0.0
TBM (μg/L)	468.6±15.1	DBCAA (μg/L)	16.7±0.6
THM ₄ (μg/L)	527.4±17.2	TBAA (μg/L)	87.6±4.6
MCAA (μg/L)	ND	HAA ₉ (μg/L)	184.5±1.0
MBAA (μg/L)	5.0±0.2	TOCl (μg/L as Cl)	32.6±4.2
DCAA (μg/L)	2.0±0.1	TOBr (μg/L as Cl)	551.1±5.8
TCAA (μg/L)	0.6±0.0	TOX (μg/L as Cl)	583.7±1.6
DBAA (μg/L)	62.7±3.5		

“ND” means “not detected”.

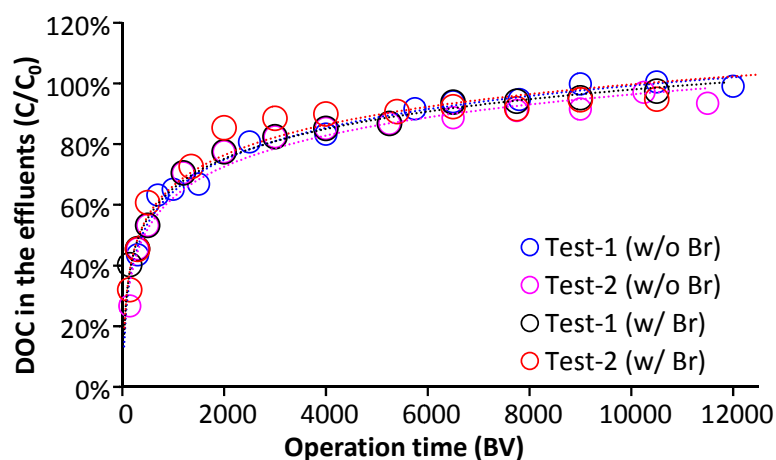


Figure S1. Column reproducibility test results with virgin Calgon F300 and SRNOM (3 mg/L as C). Lines show the logarithmic fits to the data for the comparison purpose.

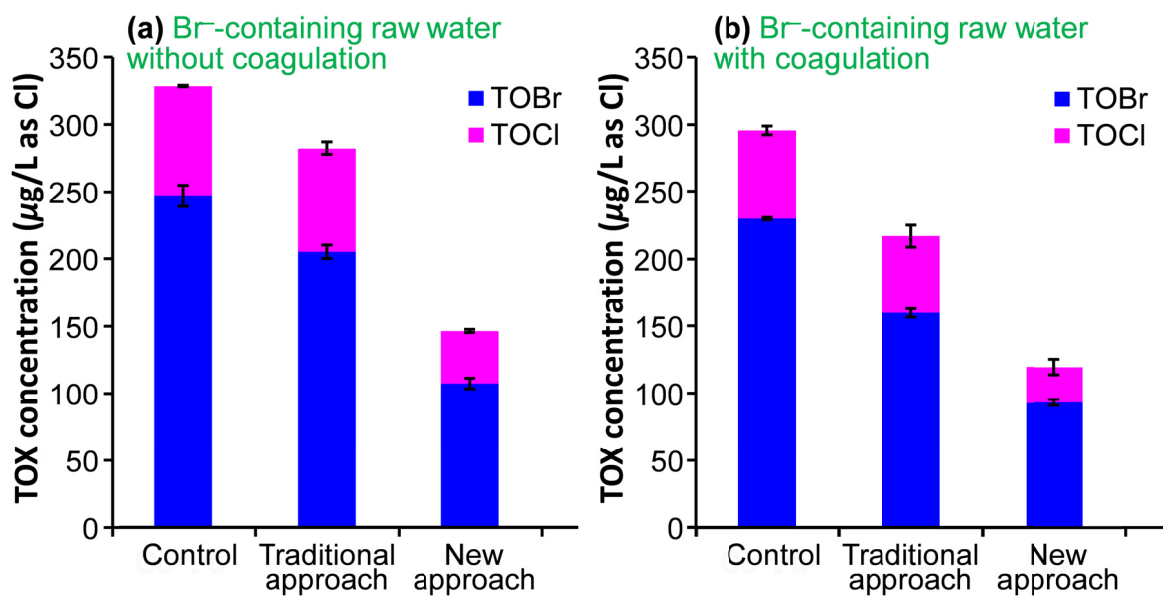


Figure S2. TOX levels in (a) non-coagulated and (b) coagulated raw water samples with chlorination only (control), with the traditional approach, and with the new approach.

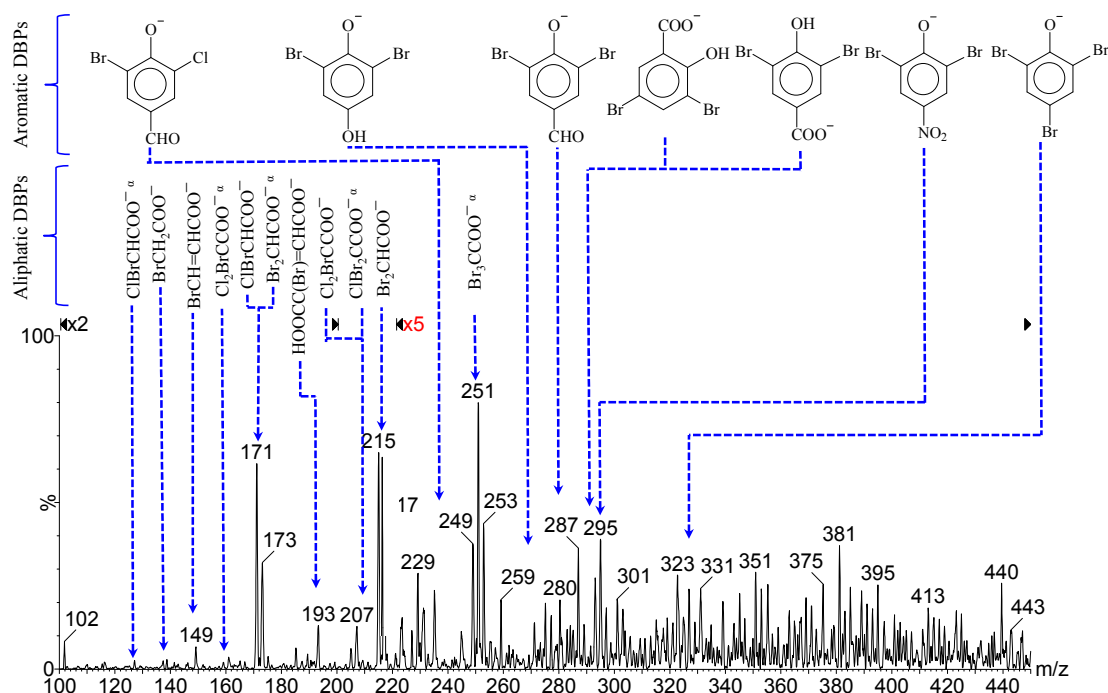


Figure S3. ESI-tqMS PIS spectrum of m/z 79 of the bromide-containing influent sample with the new approach. “ $\times 2$ ” indicates that the spectrum in m/z range of 100–200 was magnified by 2 times and “ $\times 5$ ” indicates that the spectrum in m/z range of 220–450 was magnified by 5 times.

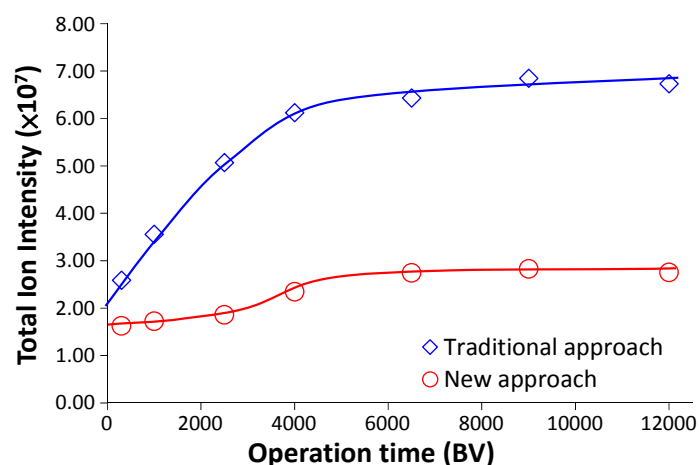


Figure S4. TII values of bromide-containing effluents with the new and traditional approaches. To reflect all the polar brominated DBPs, TII value was calculated through the summation of ion intensity from m/z 80 to 600 in the ESI-tqMS PIS spectrum of m/z 79.

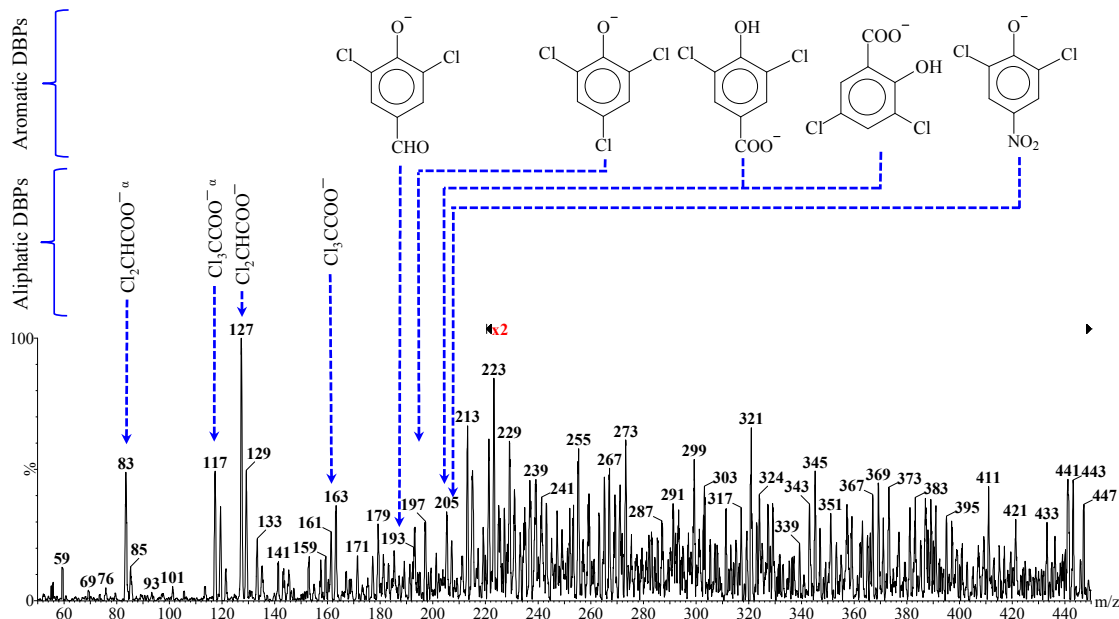


Figure S5. ESI-tqMS PIS spectrum of m/z 35 of the bromide-free influent sample with the new approach. “ $\times 2$ ” indicates that the spectrum in m/z range of 220–450 was magnified by 2 times.

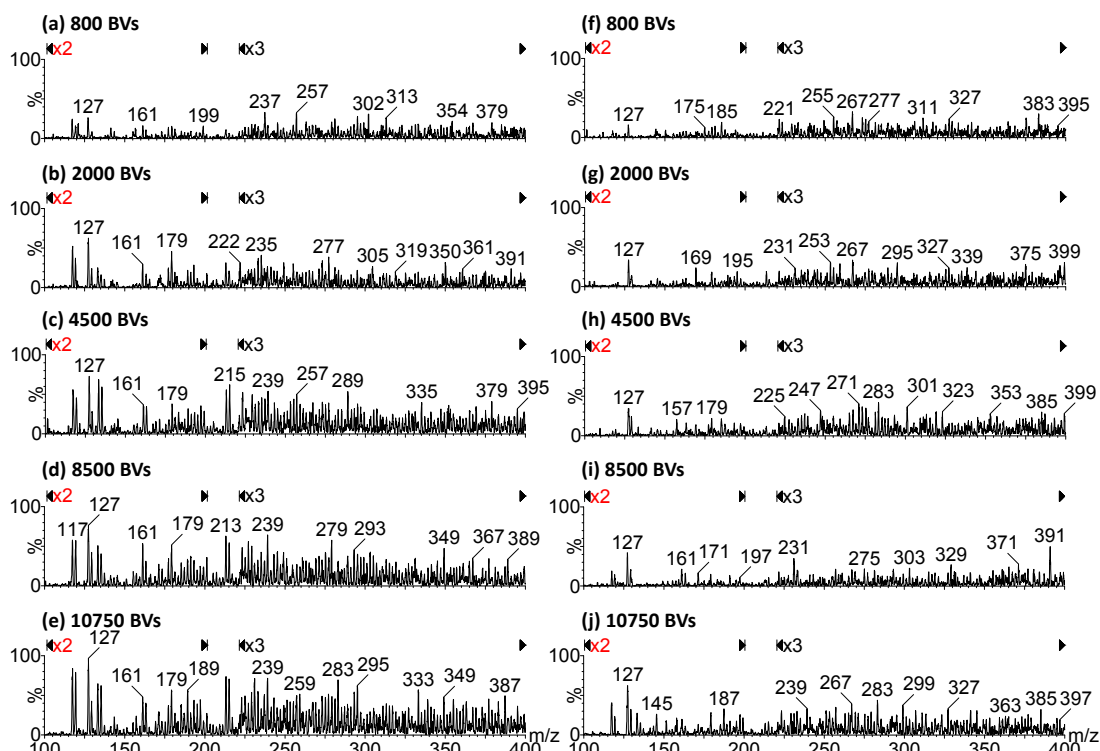


Figure S6. ESI-tqMS PIS spectra of m/z 35 of the bromide-free effluent samples with the traditional approach collected at (a) 800 BVs, (b) 2000 BVs, (c) 4500 BVs, (d) 8500 BVs, and (e) 10750 BVs, respectively; ESI-tqMS PIS spectra of m/z 35 of the bromide-free effluent samples with the new approach collected at (f) 800 BVs, (g) 2000 BVs, (h) 4500 BVs, (i) 8500 BVs, and (j) 10750 BVs, respectively. The y-axes are on the same scale with a maximum intensity of 6.40×10^5 . “ $\times 2$ ” in charts a–j indicates that the spectra in m/z range of 100–200 were magnified by 2 times and “ $\times 3$ ” in charts a–j indicates that the spectra in m/z range of 220–400 were magnified by 3 times.

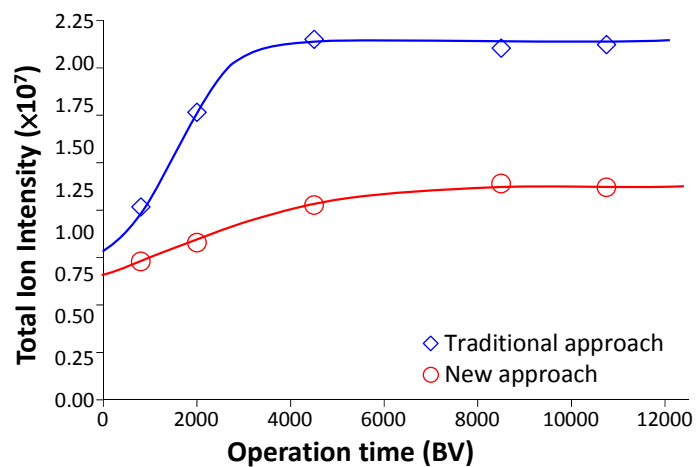


Figure S7. TII values of bromide-free effluents with the new and traditional approaches. To reflect all the polar chlorinated DBPs, TII value was calculated through the summation of ion intensity from m/z 36 to 600 in the ESI-tqMS PIS spectrum of m/z 35.

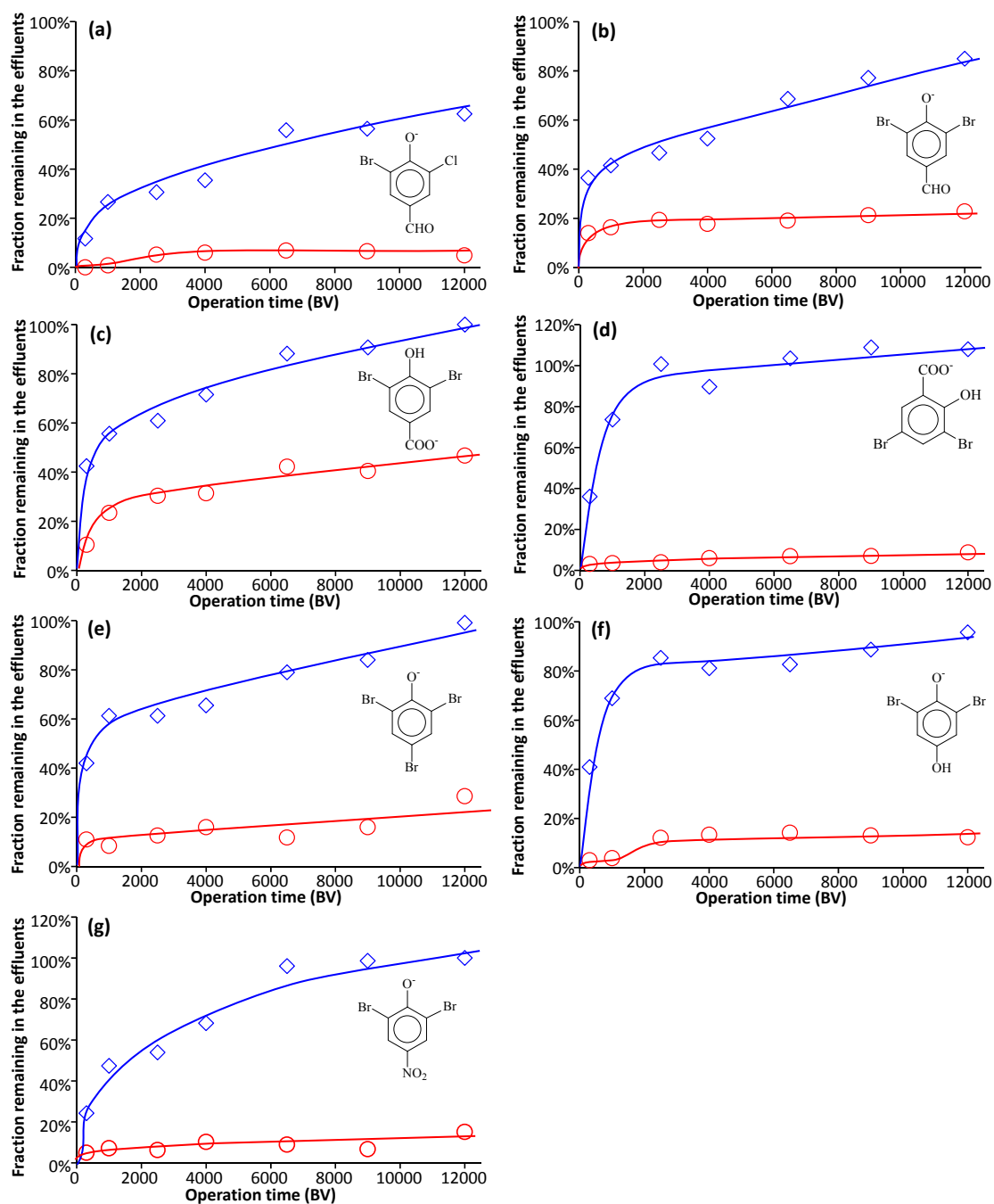


Figure S8. Normalized peak areas of (a) 3-bromo-5-chloro-4-hydroxybenzaldehyde, (b) 3,5-dibromo-4-hydroxybenzaldehyde, (c) 3,5-dibromo-4-hydroxybenzoic acid, (d) 3,5-dibromosalicylic acid, (e) 2,4,6-tribromophenol, (f) 2,6-dibromo-1,4-hydrobenzoquinone, and (g) 2,6-dibromo-4-nitrophenol in the UPLC/ESI-tqMS MRM chromatograms of the bromide-containing effluent samples with the traditional approach (◇) and the new approach (○).

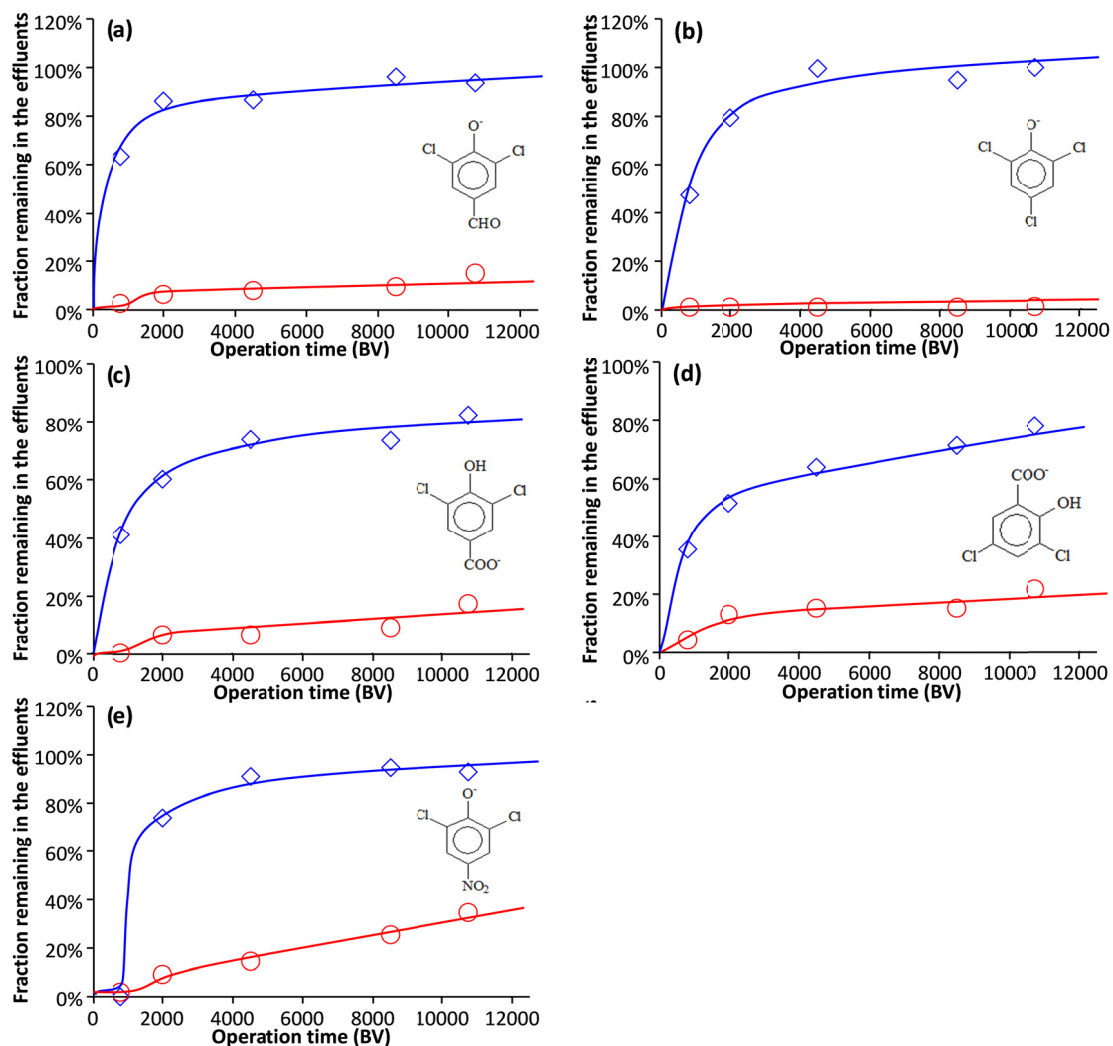


Figure S9. Normalized peak areas of (a) 3,5-dichloro-4-hydroxybenzaldehyde, (b) 2,4,6-trichlorophenol, (c) 3,5-dichloro-4-hydroxybenzoic acid, (d) 3,5-dichlorosalicylic acid, and (e) 2,6-dichloro-4-nitrophenol in the UPLC/ESI-tqMS MRM chromatograms of the bromide-free effluent samples with the traditional approach (◇) and the new approach (○).

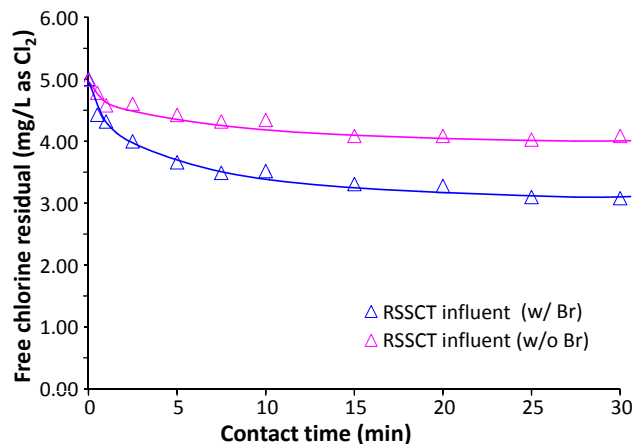


Figure S10. The free chlorine residual decay curves of the bromide-containing and bromide-free influents.

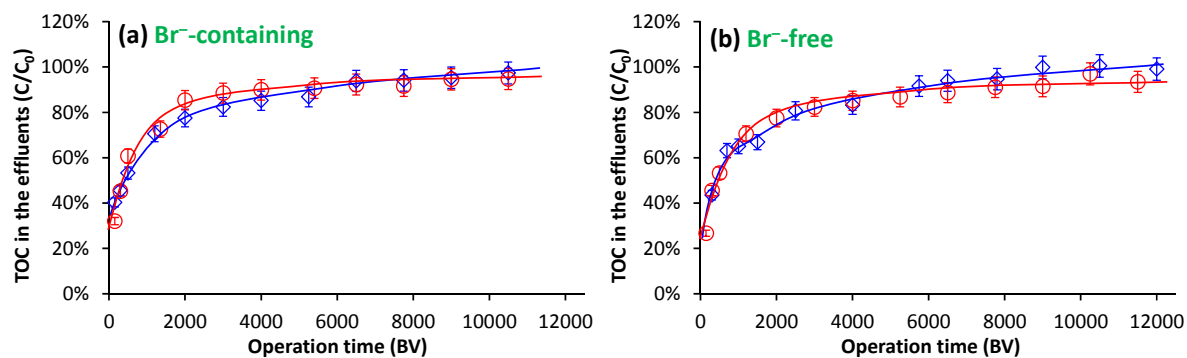


Figure S11. The breakthrough profiles of DOC level in the effluent samples with the traditional approach (◇) and the new approach (○): (a) treatment of the bromide-containing simulated raw water, and (b) treatment of the bromide-free simulated raw water.